Treatment of Small-Cell Lung Cancer Xenografts with Iodine-131-Anti-Neural Cell Adhesion Molecule Monoclonal Antibody and Evaluation of Absorbed Dose in Tissue

Makoto Hosono, Keigo Endo, Masako N. Hosono, Hisataka Kobayashi, Makoto Shirato, Harumi Sakahara, Ryuzo Ueda and Junji Konishi

Department of Nuclear Medicine, Kyoto University Faculty of Medicine, Kyoto; Department of Nuclear Medicine, Gunma University School of Medicine, Gunma; Department of Radiology, Osaka City University School of Medicine, Osaka; and Laboratory of Chemotherapy, Aichi Cancer Center, Aichi, Japan

Human small-cell lung cancer (SCLC) is considered a feasible target for immunotherapy using a radiolabeled monoclonal antibody (Mab). A murine Mab, NE150 (IgG1), reacts with the neural cell adhesion molecule, which is identical to cluster 1 antigen of SCLC. **Methods:** To estimate their therapeutic effects, NE150 and an isotype-matched control Mab were labeled with ^{131}I and administered intravenously as a single dose into athymic mice inoculated with a NCI-H69 SCLC xenograft. The absorbed dose in organs was also examined based upon a long-term biodistribution study of ^{131}I-NE150. **Results:** Tumors (initial volume 563.4 ± 223.5 mm^3) treated with 11.1 MBq (300 μCi) of ^{131}I-NE150 diminished and became invisible at days 30–33, demonstrating a 60-day mean growth delay to reach a tripled initial volume compared with sham-treated tumors. Cumulative absorbed doses were estimated to be 2310, 410, 500, 330, and 790 cGy for the tumor, liver, kidney, spleen and lung, respectively. **Conclusion:** Iodine-131-NE150 had potent therapeutic effects against SCLC transplants in athymic mice, however, careful assessment of the side effects, improvement of radioiodination and chimerization of the Mab might be necessary to achieve efficient targeting in clinical therapeutic applications.

Key Words: radiolabeled monoclonal antibody; small cell lung cancer xenografts

J Nucl Med 1994; 35:296–300

Small-cell lung cancer (SCLC), characterized by endocrine, features a tendency for metastasizing and high chemo- and radiosensitivity, represents 20%–25% of lung cancers (*1*). As most post-therapy patients undergo recurrence and tumors become refractory to repeated therapy, antibody-guided radiotherapy has been considered as a further therapeutic strategy. Several reports have described animal studies of SCLC therapy using radiolabeled monoclonal antibodies (Mabs) reactive with some SCLC-related antigens (*2–4*). The neural cell adhesion molecule (NCAM) is considered the most specific among the SCLC-related antigens. Since most SCLC tumors express NCAM on the surface membrane of the cells (*5*), it is thought to be an optimal target for radioimmunodetection or therapy.

Mab NE150, one of the cluster 1 antibodies registered in the First and Second International Workshops on Small Cell Lung Cancer Antigens (*6,7*), recognizes one of the epitopes on NCAM. At least three epitopes are present on the molecule (*8*). NCAM is expressed in human normal tissues such as nerves, endocrine glands, and NK cells (*5*). This study was performed to determine the potency of ^{131}I-labeled Mab in treating transplanted SCLC tumors in athymic mice, where the volume of tumor was large enough to simulate SCLC lesions in humans. In addition, to estimate the absorbed dose in mice receiving therapeutic dose of ^{131}I-NE150, the biodistribution was examined along with the diminution of tumors up to 21 days after administration.

MATERIALS AND METHODS

Cell Line and Xenografts

The SCLC cell line NCI-H69 (*9*) was cultured in RPMI 1640 culture medium (Gibco, Grand Island, NY) supplemented with 1 m*M* glutamine and 10% fetal calf serum. For the studies in mice, NCI-H69 SCLC cells were implanted by subcutaneous inoculation of a tumor mince into the flanks of 5–7-wk-old female BALB/c nu/nu mice. Xenografted mice were used when the tumor volumes reached approximately 500 mm^3, 2–3 wk after inoculation.

Monoclonal Antibody and Radiolabeling

Murine Mab NE150 (IgG1) that recognizes the human neural cell adhesion molecule was obtained by immunizing BALB/c mice with primary neuroblastoma cells (*10*). Murine Mab 59A that is reactive with human thyroglobulin was used as an isotype-

Received Apr. 2, 1993; revision accepted Sept. 22, 1993.

For correspondence and reprints contact: Makoto Hosono, MD, Dept. of Nuclear Medicine, Kyoto University Hospital, Shogoin, Sakyo-ku, Kyoto 606-01, Japan.

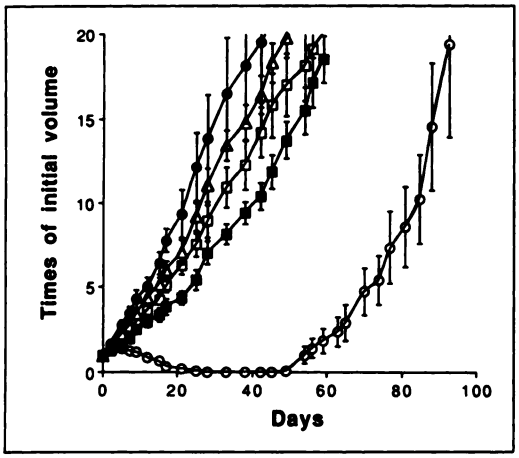

FIGURE 1. Changes in the size of NCI-H69 xenografts after radioimmunotherapy. Five groups of mice (six mice/group) were treated with 11.1 MBq (○) and 3.7 MBq of ^{131}I-NE150 (□), unlabeled NE150 (△), 11.1 MBq of ^{131}I-59A (■) or sham-treated (●). Error bars indicate 1 s.e.

matched control Mab. They were purified from mouse ascites fluid using MabTrap G (Pharmacia LKB Biotechnology, Uppsala, Sweden). Mabs were labeled with ^{125}I or ^{131}I using the chloramine-T method (*11*). For the Scatchard analysis, NE150 (40 μg) in 0.3 *M* phosphate-buffer, pH 7.5, and ^{125}I (14.8 MBq) for protein labeling (Amersham International, Buckinghamshire, UK) were mixed with 2.5 μg of chloramine-T (Nakarai Chemicals, Kyoto, Japan). After 5 min, radiolabeled NE150 was separated from free iodine through PD-10 gel chromatography (Pharmacia LKB Biotechnology). For therapeutic experiments, 800 μg of Mabs and 296 MBq (8 mCi) of NaI-131 (E. I. DuPont de Nemours & Co. Inc., Wilmington, DE) were mixed with 6 μg of chloramine-T in 0.3 *M* phosphate-buffer, pH 7.5. After 5 min, ^{131}I-labeled Mabs were separated from free ^{131}I by PD-10 gel chromatography. The specific activity of the ^{131}I-labeled NE150 was 207–244 MBq/mg, and that of ^{131}I-59A was 185–200 MBq/mg.

Scatchard Analysis

Iodine-125-labeled NE150 was incubated with 1×10^7 NCI-H69 cells for 1 hr at 4°C, and the radioactivity bound to the cells was counted. The binding affinity constant was calculated by means of a Scatchard analysis (*12*).

Radioimmunotherapy

Four of five groups (six mice/group) of mice received an intravenous injection of 11.1 or 3.7 MBq of ^{131}I-labeled NE150, unlabeled NE150 and 11.1 MBq of ^{131}I-labeled 59A, while the fifth group was sham-treated. The initial tumor volume was 563.4 ± 223.5 mm^3 in all mice; and 546.6 ± 163.3, 522.1 ± 215.8, 502.1 ± 143.8, 571.6 ± 290.7 and 674.9 ± 230.3 mm^3 in the 11.1 MBq of ^{131}I-NE150, 3.7 MBq of ^{131}I-NE150, unlabeled NE150, 11.1 MBq of ^{131}I-59A, and sham-treated groups, respectively. The Mab dose was adjusted to 70 μg per mouse by adding unlabeled NE150 or 59A. The mice were given water containing 0.1% potassium iodide to inhibit the uptake of released radioiodine into the thyroid and were housed in a clean isolator. The short and long axes of the xenografts were measured 2–3 times/wk with a caliper, and the tumor volume was calculated using the formula:

$$\pi/6 * (\text{short-axis})^2 * (\text{long-axis}).$$

Biodistribution and Estimation of Absorbed Dose in Treated Mice

To estimate the absorbed dose in the treated mice, six groups (four mice per group) of mice bearing tumors similar in weight to those used for the radioimmunotherapy studies (436.3 ± 170.5 mm^3), received an intravenous injection of 11.1 MBq/70 μg of ^{131}I-labeled NE150. They were killed at Days 1, 2, 4, 7, 14 and 21, then the tumors and organs were weighed and the radioactivity was counted using a gamma counter. Data were expressed as percentages of injected dose per gram of tissue. Absorbed doses in tumor and organs were calculated from the biodistribution data with an integrated single exponential curve fit of the time activity using the software CA-CRICKET Graph (Computer Associates, San Diego, CA). The calculation was based on the method in the MIRD pamphlet (*13*). Only beta particle irradiation was considered because the mean range of the beta particle represents 95% deposition within 0.99 mm, and gamma emission passes through mice with only a little absorption. To monitor peripheral blood cell counts, blood was taken from the hearts of mice upon sacrifice, using dipotassium ethylenediaminetetraacetic acid (K_2 EDTA) as an anticoagulant at Days 0, 7, 14, 21 and 60. Peripheral red cells, white cells and platelets were counted manually using a standard Bürker-Türk counting chamber (Erma Inc., Tokyo, Japan) and a microscope. The blood was diluted in Gowers', Türk's, and Rees-Ecker's solutions for red cells, white cells and platelets, respectively.

RESULTS

Scatchard analysis of the binding of NE150 to NCI-H69 cells indicated an affinity constant of $1.2 \times 10^8\ M^{-1}$ and binding sites numbering 6.2×10^4 per cell.

The change in tumor volume in response to the treatment regimens is illustrated in Figure 1. Six NCI-H69 SCLC xenografts treated with a single dose of 11.1 MBq of ^{131}I-NE150 shrank and became invisible at days 30–33. The period that the athymic mice remained tumor-free ranged from 7 to 21 days (13.2 ± 5.6 days). Treatment with 3.7 MBq of ^{131}I-NE150 or 11.1 MBq of ^{131}I-59A resulted in only a partial inhibition of tumor growth (5456.0 ± 1804.4 mm^3, 4749.9 ± 2516.5 mm^3, respectively, at Day 33), while unlabeled NE150 had no inhibitory effect on tumor growth (6769.0 ± 2366.8 mm^3 at Day 33) compared with sham-treatment (9498.0 ± 815.1 mm^3 at Day 33) (Fig. 1). When plotted on a semilog scale, the curves were nearly linear from 1 to 5 times of initial tumor volume and the growth delay assessment of the tumors was expressed as days required for tumors to reach three times the initial volume (Table 1). Therapy with 11.1 MBq of ^{131}I-NE150 produced a 60-day mean growth delay, which was statistically different from sham treatment. Administration of 11.1 MBq of ^{131}I-59A resulted in an eight-day growth delay, whereas 3.7 MBq of ^{131}I-NE150 and unlabeled NE150 showed no statistically significant growth delay.

The absolute levels of radioactivity in tumors and organs at Days 1, 2, 4, 7, 14 and 21 are presented in Table 2. Tumor uptake reached 11.2% at Day 2, and the tumor-to-blood ratio was 0.93 ± 0.24, 1.27 ± 0.26, 1.65 ± 0.58,

TABLE 1
Growth Delay Analysis of NCI-H69 SCLC Xenografts in Mice

Treatment	Days for tumor to reach 3 times the initial volume
11.1 MBq NE150	68.0 ± 8.9*
3.7 MBq NE150	10.5 ± 2.7†
unlabeled NE150	8.1 ± 1.9†
11.1 MBq 59A	14.1 ± 4.7*
Control	6.1 ± 1.9

*$p < 0.01$.
†Not significant.

TABLE 3
Estimates of Absorbed Radiation Dose in Tissues Calculated on the Basis of the Biodistribution Data in Mice Treated with 11.1 MBq of ^{131}I-NE150

Organ	Absorbed dose (cGy)		
	Up to day 7	Up to day 30	total
Liver	350	410	410
Kidney	390	500	500
Spleen	240	330	330
Lung	650	790	790
Femur	130	160	160
Tumor	1480	2280	2310

2.50 ± 0.50, 2.17 ± 1.04 and 8.71 ± 2.41 on Days 1, 2, 4, 7, 14 and 21, respectively.

Dosimetric estimations in the tumor, liver, spleen, kidney, lung and femur are summarized in Table 3. Most irradiation was accomplished by Day 7, however, the irradiation to tumor was prolonged and the absorbed radiation dose was estimated as 2310 cGy per 11.1 MBq of ^{131}I-NE150.

The peripheral blood cell counts are shown in Figure 2. After reaching the nadir in the white cell and platelet counts at Day 14, there was spontaneous recovery of the hematopoietic function. The number of red cells did not significantly drop.

DISCUSSION

Since NCAM is usually expressed in SCLC, it is an optimal target of radioimmunotherapy. In this study, we observed the complete shrinkage of xenografted SCLC of 547 mm^3 after administering 11.1 MBq of ^{131}I-NE150. This indicates that SCLC patients with metastatic nodules as large as these xenografts may be effectively treated with ^{131}I-NE150.

Iodine-131 has a maximum beta energy of 0.608 MeV, a 95% deposition range of 0.99 mm and offers the advantages of a long history of clinical use, commercial availability and gamma emission employed for body imaging, although its dehalogenation in vivo due to the lability of the o-iodotyrosil label reduces the accumulation of radioactivity in organs (*14*).

The distribution of radiolabeled Mab in mice administered with a therapeutic dose of Mab may differ from that with a tracer-dose of Mab because of rapid tumor growth of SCLC xenografts and tumor degradation as the result of therapy (*15*). Therefore, mice given therapeutic doses of Mab were examined to estimate the absorbed radioactivity. Tumors absorbed a dose of 2310 cGy/11.1 MBq, which is similar to that in the previous report of Beaumier et al., who treated SCLC xenografts in mice with ^{186}Re-labeled Mab and estimated the absorbed dose in tumor as 2175 cGy/240 μCi (*3*).

The lung is one of the most irradiated normal organs. Iodine-131-NE150 in the blood might contribute to the irradiation of the lung since lung radioactivity paralleled that of the blood. Patients with SCLC who received chemotherapy or external irradiation, are sensitive to lung irradiation, which may cause radiation pneumonitis. Therefore, it will be important to estimate the absorbed dose in the lung when patients undergo immunoscintigraphy with ^{131}I-NE150.

Normal tissues expressing NCAM on cell surface membranes but not protected by the blood-brain barrier (the peripheral nerve, adrenal and thyroid glands), may suffer from irradiation when exposed to a therapeutic dose. An antibody to a melanoma cell showing affinity to nerve tissue caused pain in patients in a melanoma immunotherapy study by Saleh et al. (*16*). NE150 reacts with human but

TABLE 2
Biodistribution of ^{131}I-NE150 in Athymic Mice Bearing NCI-H69 Tumors Treated with a Therapeutic Dose

Organs	%ID/g of tissue					
	Day 1	Day 2	Day 4	Day 7	Day 14	Day 21
Blood	13.81 ± 2.78	9.10 ± 2.39	6.37 ± 3.30	3.06 ± 1.30	2.38 ± 0.82	0.41 ± 0.04
Liver	4.14 ± 1.01	2.99 ± 1.15	1.65 ± 0.40	0.59 ± 0.23	0.62 ± 0.27	0.09 ± 0.00
Kidney	4.57 ± 1.58	3.75 ± 1.08	1.57 ± 0.48	0.95 ± 0.45	0.81 ± 0.21	0.12 ± 0.01
Intestine	1.53 ± 0.60	1.31 ± 0.63	0.41 ± 0.12	0.29 ± 0.15	0.25 ± 0.16	0.04 ± 0.01
Stomach	3.73 ± 2.41	3.30 ± 1.44	0.33 ± 0.04	0.64 ± 0.18	0.39 ± 0.20	0.11 ± 0.04
Spleen	3.62 ± 1.55	2.96 ± 0.78	1.00 ± 0.48	0.56 ± 0.29	0.48 ± 0.26	0.07 ± 0.01
Lung	7.09 ± 2.43	5.57 ± 1.74	2.66 ± 1.06	1.53 ± 0.72	1.46 ± 0.61	0.19 ± 0.01
Muscle	0.68 ± 0.20	0.74 ± 0.11	0.38 ± 0.25	0.18 ± 0.07	0.16 ± 0.03	0.02 ± 0.00
Femur	1.57 ± 0.50	1.39 ± 0.37	0.39 ± 0.17	0.29 ± 0.22	0.32 ± 0.15	0.03 ± 0.01
Tumor	11.64 ± 1.89	11.26 ± 2.25	9.24 ± 2.40	7.25 ± 2.01	4.59 ± 1.30	3.62 ± 1.21

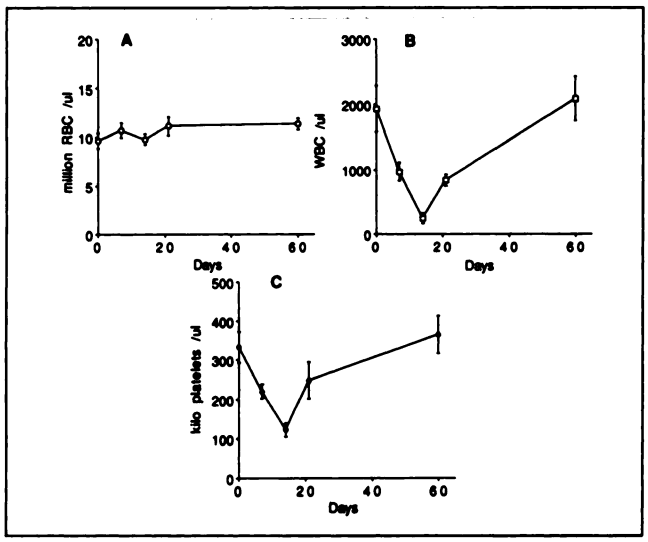

FIGURE 2. Peripheral blood cell counts in xenografted mice at Days 0, 7, 14, 21, 60 (n = 4). Error bars indicate 1 s.d. (A), red blood cells (B), white blood cells and (C), platelets.

not with murine NCAM. However, major organs such as the liver, kidney, lung and bowel in humans do not express NCAM (*5*). Thus, the absorbed radioactivity in murine organs helps to estimate those in the human.

As natural killer (NK) cells have the CD56 antigen identical to NCAM (*8*) on the surface membrane, radiolabeled NE150 may affect their activity. Antibody-guided irradiation may not completely kill the tumor cells, and the host immune system may play an important role in eliminating tumor cells surviving after irradiation. According to some reports, in most human subjects the cytotoxic function of NK cells against sensitive tumor cells is abrogated by gamma irradiation in vitro at a dose of 30 Gy (*17,18*). Thus, the affinity of NE150 to NK cells represents a disadvantage in cancer therapy.

In our study, the counts of white blood cells and platelets decreased as the result of irradiation to hematopoietic organs. Bone marrow metastases are reportedly detected in about 25%–45% of SCLC patients by conventional histological studies (*19,20*) and in 63% of SCLC patients by immunohistochemical examination (*21*). Therefore, the exposure of bone marrow to antibody-guided irradiation seems inevitable in order to eliminate malignant cells within it. Autologous bone marrow transplantation with ex vivo antibody therapy may be necessary for efficient human therapy.

Meanwhile, the dose of 11.1 MBq (300 μCi)/70 μg in a mouse is equivalent to approximately 27.75 GBq (750 mCi)/175 mg, or 4.44 GBq (120 mCi)/28 mg on the basis of body weight or body surface area in humans. In order to administer such a large amount of radiolabeled Mab, repeated infusion may be needed. Chimerization of Mab NE150 should reduce the generation of human anti-murine antibody during multiple administrations of Mab (*22,23*). Side effects due to specific binding to normal tissues such as peripheral nerves, NK cells and the adrenal medulla, must be carefully assessed in clinical application. Improvement of radioiodination such as *N*-succinimidyl-3-(tri-*n*-butylstannyl) benzoate (ATE) method, may enhance the tumor localization (*24,25*), but ^{131}I-labeled NE150 is a candidate for efficient radioimmunotherapy of SCLC.

REFERENCES

1. Minna JD. Neoplasm of the lung. In: Braunwald E, Isselbacher KJ, Petersdorf RG, Wilson JD, Martin JB, Fauci AS, eds. *Harrison's principles of internal medicine, 11th edition*. New York: McGraw-Hill Book Company; 1987;1115–1123.
2. Yoneda S, Fujisawa M, Watanabe J, et al. Radioimmunotherapy of transplanted small cell lung cancer with ^{131}I-labeled monoclonal antibody. *Br J Cancer* 1988;58:292–295.
3. Beaumier PL, Venkatesan P, Vanderheyden J-L, et al. Rhenium-186 radioimmunotherapy of small cell lung carcinoma xenografts in nude mice. *Cancer Res* 1991;51:676–681.
4. Smith A, Waibel R, Stahel RA. Selective immunotherapy of small cell cancer xenografts using ^{131}I-labelled SWA11 antibody. *Br J Cancer* 1991; 64:263–266.
5. Takahashi T, Ueda R, Song X, et al. Two novel cell surface antigens on small-cell lung carcinoma defined by mouse monoclonal antibodies NE-25 and PE-35. *Cancer Res* 1986;46:4770–4775.
6. Beverly PCL, Souhami RL, Bobrow LG. Results of the central data analysis. *Lung Cancer* 1988;4:15–36.
7. Souhami R, Beverley P, Bobrow L, Lendermann J. Antigens of lung cancer: results of the second international workshop on lung cancer antigens. *J Natl Cancer Inst* 1991;83:609–612.
8. Hida T, Koike K, Sekido Y, et al. Epitope analysis of cluster 1 and NK cell-related monoclonal antibodies. *Br J Cancer Suppl* 1991;14:24–28.
9. Gazdar AF, Carney DN, Russell EK, et al. Establishment of continuous, clonable cultures of small-cell carcinoma of the lung which have amine precursor uptake and decarboxylation cell properties. *Cancer Res* 1980;40: 3502–3507.
10. Ueda R, Takahashi T, Watanabe H, et al. Serological and biochemical analysis of four antigens associated with small cell lung cancer. *Lung Cancer* 1988;4:96–98.
11. Greenwood FC, Hunter WM, Glover JS. The preparation of ^{131}I-labelled human growth hormone of high specific radioactivity. *Biochem J* 1963;89: 114–123.
12. Scatchard G. The attraction of proteins for small molecules and ions. *Ann NY Acad Sci* 1949;51:660–672.
13. Berger MU. Distribution of absorbed dose around point sources of electrons and beta particles in water and other media. Medical internal radiation dose (MIRD) pamphlet no. 7. *J Nucl Med* 1971;12(suppl):7–23.
14. Carrasquillo JA, Mulshine JL, Bunn PAJ, et al. Indium-111 T101 monoclonal antibody is superior to iodine-131 T101 in imaging of cutaneous T-cell lymphoma. *J Nucl Med* 1987;28:281–287.
15. Lee Y, Bullard D, Zalutsky M, et al. Therapeutic efficacy of antiglioma mesenchymal extracellular matrix ^{131}I-radiolabeled murine monoclonal antibody in a human glioma xenograft model. *Cancer Res* 1988;48:559–566.
16. Saleh MN, Khazaeli MB, Wheeler RH, et al. Phase I trial of the murine monoclonal anti-GD2 antibody 14G2a in metastatic melanoma. *Cancer Res* 1992;53:4342–4347.
17. Zarcone D, Tilden AB, Lane VG, Grossi CE. Radiation sensitivity of resting and activated nonspecific cytotoxic cells of T lineage and NK lineage. *Blood* 1989;73:1615–1621.
18. Rana R, Vitale M, Mazzotti G, Manzoli L, Papa S. Radiosensitivity of human natural killer cells: binding and cytotoxic activities of natural killer cell subsets. *Radiat Res* 1990;124:96–102.
19. Hansen HH, Muggia FM, Selawry OS. Bone marrow examination in 100 consecutive patients with bronchogenic carcinoma. *Lancet* 1971;2:443–445.
20. Skov BG, Hirsch FR, Bobrow L. Monoclonal antibodies in the detection of bone marrow metastases in small cell lung cancer. *Br J Cancer* 1992;65: 593–596.
21. Berendsen HH, Leij LDE, Postmus PE, Harr JCT, Poppema S, The TH. Detection of small cell lung cancer metatases in bone marrow aspirates using monoclonal antibody directed against neuroendocrine differentiation antigen. *J Clin Pathol* 1988;41:273–276.

22. Hosono M, Endo K, Sakahara H, et al. Human/mouse chimeric antibodies show low reactivity with human anti-murine antibodies (HAMA). *Br J Cancer* 1992;65:197–200.
23. Sands H. Radiolabeled monoclonal antibodies for cancer therapy and diagnosis: is it really a chimera? *J Nucl Med* 1992;33:29–32.
24. Zalutsky M, Noska M, Colapinto E, Garg P, Binger D. Enhanced tumor localization and in vivo stability of a monoclonal antibody radioiodinated using N-succinimidyl 3-(tri-n-butylstannyl) benzoate. *Cancer Res* 1989;49: 5543–5549.
25. Schuster J, Garg P, Binger D, Zalutsky M. Improved therapeutic efficacy of a monoclonal antibody radioiodinated using N-succinimidyl-3-(tri-n-butylstannyl) benzoate. *Cancer Res* 1991;51:4164–4169.

EDITORIAL

The Importance of Accurate Radiation Dosimetry in Radioimmunotherapy of Cancer

The ultimate objective of radiation dosimetry in the treatment of cancer is to predict the biologic effects of energy deposited in tissue, thus allowing a physician to prescribe therapy that will benefit a patient with cancer. The role of the dosimetrist is well established in conventional radiation therapy, where there are established methods for performing dosimetric estimation and measurement, and for interpreting and applying the results to experimental and clinical cancer therapy. The role, value and methodology of radiation dosimetry in radioimmunotherapy is less well established. Although there have been efforts to standardize estimation of radiation dose in humans (*1,2*), optimal, uniform methods for dosimetric estimation and measurement, and interpretation of radiation dose, have not been commonly accepted. Dosimetric techniques suitable for application in therapeutic animal studies are even less well formulated.

In radioimmunotherapy, radiation energy is imparted at a low dose rate to tissues from internally distributed sources. Thus, the estimation of deposited radiation dose and its interpretation, will differ significantly from external radiation therapy. The total amount and rate of energy deposition in individual tissues varies by tissue and is determined by the biodistribution of the administered radionuclide and the physical characteristics of emitted particles. Biodistribution will depend on a multitude of factors, including the specificity and amount of the carrier molecule infused, the radionuclide and chemistry of conjugation to the carrier molecule, and the total amount of conjugate administered. Since radiation energy is deposited over a prolonged period, i.e., hours to days, it may be necessary to take into account any early biologic effects resulting from the radiation which might influence late biodistribution (*3*) or from associated combined modality therapy (*4*).

Once biodistribution is known, accurate estimation of absorbed radiation dose in a particular tissue will depend upon a dosimetric model that includes both the physical characteristics of the emitted particles and the specific spatial and temporal distribution of the source radionuclide compared to the target tissue. Techniques for correlating absorbed dose to biological effect, and utilizing dose estimates for extrapolating from experimental models to human patients, are still being developed. The study of Hosono et al. (*5*) exemplifies the unresolved and evolving nature of dosimetric estimation and its clinical application in radioimmunotherapy.

In the accompanying manuscript, Hosono et al. present data showing that infusion of an ^{131}I-labeled antibody, NE150, which binds to the NCAM molecule present on small cell lung cancer, can produce a greater therapeutic effect than an equivalent amount of an ^{131}I-labeled antibody that does not bind to tumor. The toxicity of this therapy is defined. Efficacy and toxicity data are accompanied by an estimate of radiation dose to the tumor and normal tissues. The authors hope that correlation of these two datasets will provide a means of comparing these results to those of other investigators, predicting the radiation dose required to produce an anti-tumor effect and the toxicity associated with therapy, and extrapolating the results in animal models to the clinical situation. How well do the techniques used by Hosono et al. (and historically by many other investigators, including ourselves) meet these objectives?

Successful interpretation of experimental studies on the effects of radiolabeled antibodies in cancer treatment requires a careful analysis of the biological distribution of the administered radionuclide in normal organs and tissues of the body, in tumors, and in circulating blood. This may be accomplished by serially sacrificing different groups of laboratory animals at several time points after the initial injection of radiolabeled antibody, and determining the amount of radionuclide in each of the major organs, tumors, and blood. The biokinetics of the radionuclide may then be evaluated for each tissue by evaluating the concentration of activity (μCi or Bq per gram) in each tissue over time through complete decay (infinite time). When the time-dependent concentrations of the radionuclide in individual tissues are known, further assessments may be made to determine cumulated activities and radiation absorbed doses.

Investigators usually decay-correct the tissue-count data with an appropriate counting standard to infer the concentration of the antibody in tissue with time. This is commonly referred

Received Nov. 15, 1993; accepted Nov. 15, 1993.
For correspondence or reprints contact: Darrell R. Fisher, PhD, Dosimetric Modeling Group, Battelle, Pacific Northwest Laboratories, Battelle Blvd., P.O. Box 999 (K3-53), Richland, WA 99352.